Talanta 212 (2020) 120806

Contents lists available at ScienceDirect

Talanta

journal homepage: www.elsevier.com/locate/talanta

Modification of electrodes with *N*-and *S*-doped carbon dots. Evaluation of the electrochemical response

Marta Bonet-San-Emeterio[a], Manuel Algarra[b,**], Marijana Petković[b], Manel del Valle[a,*]

[a] Sensors and Biosensors Group, Department of Chemistry, Universitat Autònoma de Barcelona, 08193, Bellaterra, Barcelona, Spain
[b] CQM-Centro de Química da Madeira, Universidade da Madeira, Campus da Penteada, 9020-105, Funchal, Portugal

ARTICLE INFO

Keywords:
Modified electrode
Voltammetry
N-doped carbon dots
S-doped carbon dots
Nanomaterial
Electrochemical sensor

ABSTRACT

Nitrogen and sulphur-doped Carbons Dots (*N*-CDs and *S*-CDs) were synthesized by a hydrothermal method and incorporated as surface electrode modifiers to evaluate their properties for electrochemical sensing. The first task was to characterize the synthesized materials, for which different spectroscopies, scanning microscopes, mass spectrometry and elementary analysis were performed. Next, a glassy carbon electrode (GCE) was surface-modified with the doped CDs and applied to check the electrochemical signal of different organic compounds corresponding to different families. Water solubility of the doped carbon dots forced us to incorporate them in a graphite-polystyrene ink to complete the modification of electrodes. This modification needed a first activation to obtain a properly conductive surface. The organic compounds examined were salicylic acid, cysteine and ascorbic acid. The modified GCEs exhibited an enhanced sensitivity, probably caused by the increase of active surface, but in addition, signals of salicylic acid were shifted ca. 200 mV to lower potentials, what is a proof of the increase of the heterogeneous electron transfer rate, and a demonstration of an enhanced catalytic response.

1. Introduction

Carbon quantum dots, or simply, carbon dots (CDs) are an emerging new nanomaterial made essentially of carbon that can be considered small graphene nanoplatelets, or other small carbon aggregates [1]. Typical sizes involved are in the range of 10 nm, and in some aspects, may overcome problems assigned to conventional metal-semiconductor quantum dots (QDs) [2]. Among others, some advantages of this new carbon nanomaterial are their stability, water solubility, low toxicity, high fluorescence, biocompatibility and easy conjugation or functionalization chemistries [3].

Their most interesting analytical property is their photoluminescence in the VIS range, which has made this nanomaterial to be exhaustively studied in the development of new fluorometric or fluorescence quenching methods of analysis. This is so, because photoluminescence and reactivity of CDs may be tuneable by changing their size, depending on the synthesis method, and by introducing various functional groups at the graphitic sheet edges [4]. For all these, CDs are to be considered as promising applications in bio-sensing, cellular imaging, drug delivery and catalysis [5,6]. Inspired by the variety of their usage, there is a growing interest in the synthesis of new carbon dots, where they are in the forefront of new environmentally compatible, or green analytical methodologies [7].

Most of the articles present in the literature related to CDs exploit their potential alternative to conventional semiconductor QDs as fluorescent material for imaging [8–10]. In this area, CDs are playing up their importance in a number of applications, thanks to their inherent properties of hydrophilicity, stable luminescence, resistance to photobleaching, chemical stability, low cost and simple synthesis and functionalization [11–14]; these assets make them appropriate and/or ideal nanomaterials for selective imaging, catalysis or bactericide effects, among others existing research fields [3,4,15–21]. Nonetheless, CDs are gaining importance in new fields as in sensing and biosensing. For example, Praneerad et al. describes a CD fluorescent paper-based sensor for acetic acid vapour and Cu^{2+} detection [22]. Thanks to their semiconducting properties, CDs have also been successfully applied as a part of binary matrices for matrix-assisted laser desorption/ionization (MALDI) mass spectrometry of low mass biologically relevant molecules [23,24], enhancing the signal intensity.

Almost practically all the initial research was related with purely carbon-containing CDs, soon it was realized that their doping with elements such as nitrogen, sulphur, phosphorous or boron, or their

* Corresponding author. Sensors and Biosensors Group, Department of Chemistry, Universitat Autonoma de Barcelona, Edifici Cn, 08193, Bellaterra, Barcelona, Spain.
** Corresponding author.
E-mail address: manel.delvalle@uab.cat (M. del Valle).

https://doi.org/10.1016/j.talanta.2020.120806
Received 31 October 2019; Received in revised form 31 January 2020; Accepted 2 February 2020
Available online 03 February 2020
0039-9140/

Table 1
Elementary analysis (weight %) of the doped CDs prepared in this study[a].

	%C	%H	%N	%S
S-CDs	34.72 ± 0.34	3.88 ± 0.23	–	13.22 ± 0.22
N-CDs	54.98 ± 0.05	7.50 ± 0.51	10.72 ± 0.02	–

[a] Average value ± SD (n = 3).

combinations, could be used to tune their properties. Initially, the focus was put on the fluorescence emission, which could be altered from blue to green [25–27]. The nitrogen or sulphur atoms, which especially populate the surface of the CDs, may act as electron donators increasing their power, in terms of sensitivity, to interact with different analytical species. In a different application, nitrogen- and sulphur-doped carbon dots, sprayed over the tissue sections, lowered down the sensitivity of small molecules' detection by MALDI mass spectrometry imaging to the picomolar range, as demonstrated in recent work of Lin et al., thus becoming an important auxiliary agent in (bio)analytics [28].

Doped CDs may be prepared by different approaches, from small organic precursors, being microwave [29], pyrolysis [30] and hydrothermal [31–35] the preferred methods. Three main outcomes can be obtained: the surface modification/functionalization, doping with heteroatoms and therefore the control of crystallinity [36].

Concerning the use of CDs in electroanalysis, much less research has been done in this area [37,38]. This alternate use of CDs can be directly aimed to modify electrodes, alone, or in combination with other compounds; this strategy is inspired in the different uses reported for graphene, a greatly used precedent material for electrochemical sensors. One of the first works reported was a communication from Nguyen et al. in which they used a CDs-modified glassy carbon electrode for the determination of etoposide [39]. From 2018, there is also a report from our group, in which it was developed a totally functional sensor modified with CDs for the determination of dopamine and uric acid [40]. Other species determined with similar devices have been hydroquinone and catechol [41], adrenaline [42] and catecholamine type neurotransmitters [43]. As it is clear, CDs have been more widely applied in the electrochemical analysis of organic molecules than in other instances. In general, CDs may act in these oxidative determinations as multivalent redox species, able to facilitate electron transfer and to bring catalytic advantages, as it is the case with noble metal nanoparticles [38].

With respect to the use of doped CDs, even less articles can be found in the literature. Among the few, there is the electrocatalytic sensor based on boron-doped CDs for the detection of haemoglobin [44] or one sensor modified by electrodeposition with *N*-carbon quantum dots and copper oxide for the selective detection of aspirin [45]. Another recent work describes the use of *N*-doped CDs for detection of hydrogen peroxide and paracetamol [46]. In the present work we first introduce CDs doped with sulphur and nitrogen and their use as modifiers on glassy carbon electrode for the detection of salicylic acid, cysteine and ascorbic acid, where we have compared their electroanalytical behaviour, also in front of pristine CDs.

2. Experimental

2.1. Chemicals and reagents

All analytes used herein were of analytical reagent grade. The solutions were prepared using deionized water from a Milli-Q system (Millipore, Billerica, Ma, USA). Polyvinylpyrrolidone (PVP, average mol. 40,000) and Poly(4-styrenesulphonic acid) sodium salt (PSS, average mol. 1,000,000) used for *N*-doped and *S*-doped CDs synthesis, respectively, were from Merck (Darmstadt, Germany). The analytes for electrochemical measurements, ascorbic acid, salicylic acid and cysteine were from Panreac Química (Barcelona, Spain), Merck (Darmstadt, Germany) and Acros Organics (Geel, Belgium), respectively.

2.2. Carbon dots synthesis and modification

Methods described in the literature, with small modifications to adapt them to our laboratory, were used to obtain *N*-CDs and *S*-CDs [21]. Briefly, PVP and PSS (2 g), as start reagents for *N*-CDs and *S*-CDs respectively, were dissolved in H_2O (50 mL), the obtained solutions were transferred into a 50 mL Teflon lined steel reactor and made react in an oven at 180 °C for 3 h. The resulting brown aqueous solution showed a green fluorescence under UV light. For the purification of

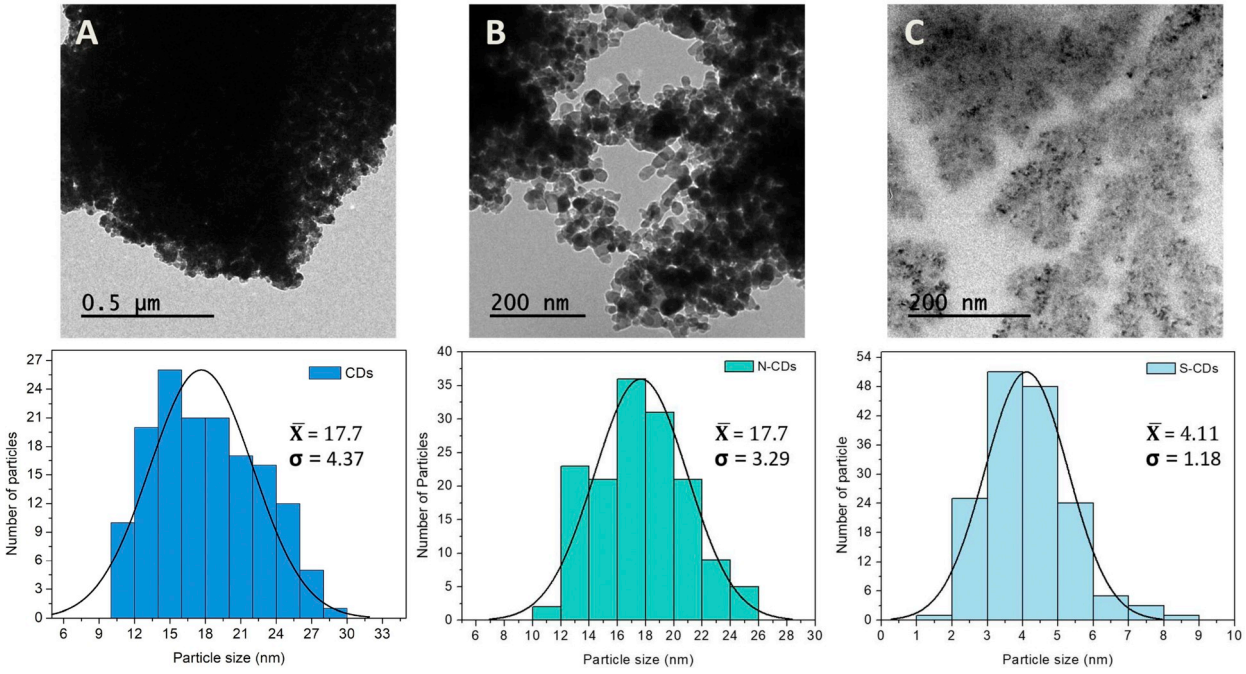

Fig. 1. SEM images and their size histograms of (A) CDs and its doped derivates: (B) *N*-CDs and (C) *S*-CDs.

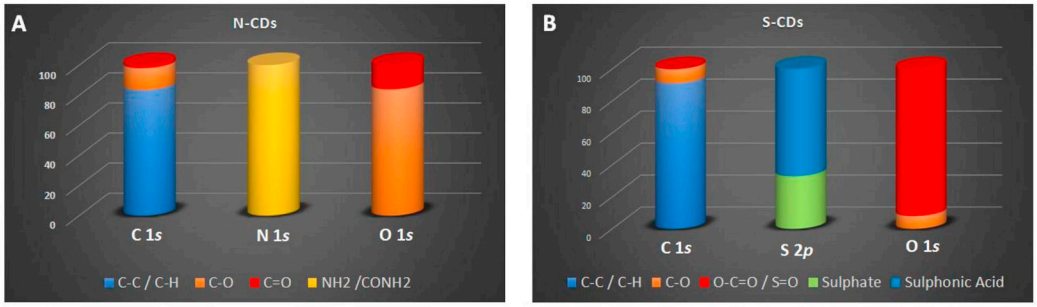

Fig. 2. Percentage of different bond types observed in the XPS analysis of the functional groups contributions for the *N*-CDs, (**A**), and the *S*-CDs, (**B**).

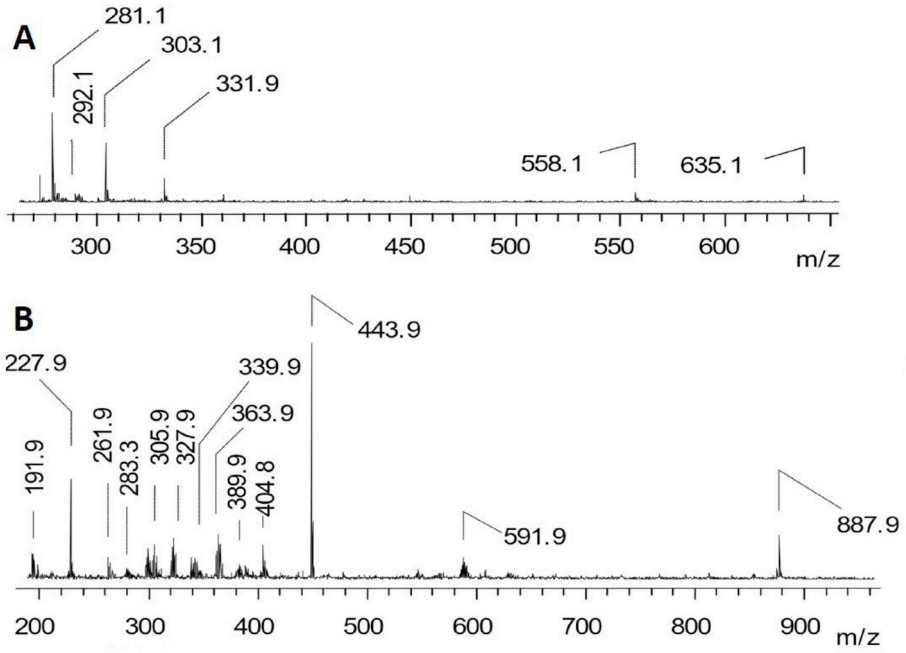

Fig. 3. Positive ion laser induced desorption and ionization time-of-flight mass spectrometry of *N*- (a) and *S*-(b) doped CDs. The spectra are acquired in reflector mode under delayed extraction conditions. Each spectrum represents the average of 2000 individual laser shots at the laser frequency of 200 Hz.

Table 2
The identity and position (*m/z*) of signals detected in the LDI TOS mass spectra of *N*-,*S*-carbon dots. All detected signals correspond to the singly-positively charged ions.

Position, *m/z*	Identity
191.9	$C_9SO_3 + 4H$
227.9	$C_{12}SO_3 + 4H$
261.9	$C_{13}SO_3 + 3H + Na$
281.1	$C_{16}(CONH_2)_2 + H$
283.9	$C_{13}SO_3 + 2H + 2Na$
292.1	$C_{17}(CONH_2)_2 + H$
303.1	$C_{16}(CONH_2)_2 + Na$
305.9	$C_{13}SO_3 + + H + 3Na$
327.9	$C_{13}SO_3 + 4Na$
331.9	$C_{17}(CONH_2)_2 + K$
339.9	$C_{14}SO_3 + 4Na$
389.9	$C_{13}(SO_3)_2 + 5H + 5Na$
443.9	$C_{13}(SO_3)_2 + 4H + 2Na + 2K$
558.1	$C_{28}(CONH_2)_4$–$2H + 2Na$
591.9	$(C_{13}SO_3 + 2H + 2Na)_2$
635.1	$C_{29}(CONH_2)_6$- + Na
887.9	$(C_{13}SO_3 + 2H + 2Na)3$

both *N*- and *S*-CDs, the obtained mixtures were centrifuged and dialyzed overnight (0.1–0.5 kDa, Biotech). Finally, both solutions were lyophilized yielding the solid *N*-CDs and *S*-CDs nanoparticles, respectively.

2.3. Characterization of doped CDs

CHNS determinations of *N*-CDs and *S*-CDs were performed by using a Thermo Scientific FLASH 2000 elemental analyser. Samples were weighed in a tin capsule and introduced into the combustion reactor via the Thermo Scientific MAS 200R autosampler, in all cases ensuring the proper amount of oxygen was present. After combustion at 1200 °C, the resultant gases were carried by a helium flow to a catalytic layer filled with copper, then swept through a GC column that separated the combustion gases, and finally detected by a thermal conductivity detector (TCD). XPS studies were carried out on a Physical Electronics PHI Versa Probe II spectrometer using monochromatic Al–K α radiation (49.1 W, 15 kV and 1486.6 eV) for analysing the core-level signals of the elements of interest with a hemispherical multichannel analyser. The sample spectra were recorded with a constant pass energy value at 29.35 eV, using a 200 μm diameter circular analysis area. The X-ray photoelectron spectra obtained were analysed using PHI Smart software

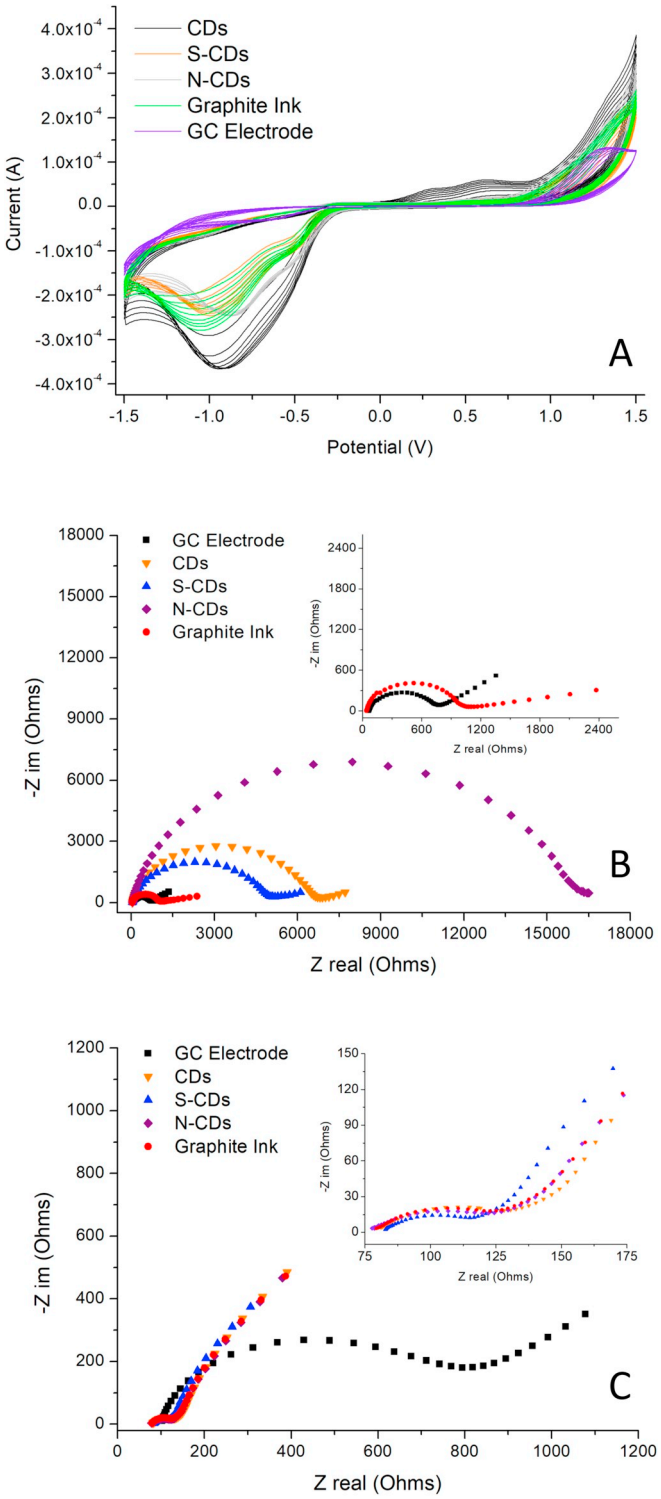

Fig. 4. Electrochemical characterization of modified GC electrodes, (A) reduction in H_2O_2 solution of the 5 studied electrodes, B and C depicts the Nyquist plots measured before the activation (B) and after the activation (C), both of them in $[Fe(CN)_6]^{3-/4-}$ solution at pH = 7.0.

and processed using the Multi Pak 9.3 package. The binding energy values were referenced to adventitious carbon C 1s signal (284.8 eV). Shirley-type background and Gauss-Lorentz peak curves were used to fit the data and determine the binding energies. Scanning electron microscopy (SEM) images were obtained using a scanning electron microscope EVO®MA10 (Zeiss, Germany) operated at 20 kV.

CDs were also characterized by matrix-assisted laser desorption/ionization time of flight mass spectrometry (MALDI TOF MS) on the Autoflex Max Device (Bruker, Bremen, Germany), equipped with the SmartBeam® laser emitting at 355 nm. Maximum laser frequency is 2 kHz, and all spectra were acquired using reflector detector and delayed extraction time 120 ns. CDs were dissolved in water at concentration of 1 mg mL^{-1}, a small volume (0.5 μL) was applied on the stainless steel MALDI target and left at room temperature for the solvent to evaporate.

2.4. Electrochemical characterization

The synthesized carbon dots were immobilized on glassy carbon electrode (GCE) using graphite-based inks. These inks were prepared using polystyrene as polymeric part and mesitylene as solvent. Concretely the mixture contained the following mass fractions: 58% of graphite, 32% of powdered polystyrene and a 10% of modifier, in this case the CDs. Once the mesitylene was added to the mixture it was homogenized by stirring it for 2 h and placing it in an ultrasonicating bath for 2 min. A GCE, previously polished using wet alumina powder from 1.0 to 0.05 μm, was modified with 5 μL of ink and dried in a 40 °C heater. Then the surface was electrochemically activated in 50 mM H_2O_2 (Merck, Darmstadt, Germany) prepared in phosphate buffer by applying 10 cyclic voltammetry (CV) cycles in a wide potential range (from +1.50 V to −1.50 V) at 0.5 V s^{-1} [47,48]. Voltammetric measurements were carried out with a MultiEmStat multichannel potentiostat controlled by MultiTrace software (both from PalmSens BV, Randhoeve, The Netherlands); a typical three electrode cell was used, formed by a combination reference electrode of Ag/AgCl (3 M KCl) and Pt counter electrode, respectively, and the working electrode designed herein. The data was recorded using the current between −1.0 and + 1.5 V with a step potential of 0.01 V and a scan rate of 50 mV s^{-1}. The solutions were made in phosphate buffer 50 mM (Merck, Darmstadt, Germany) at pH = 7.4 with 100 mM KCl as electrolyte and measured at room temperature without stirring. Electrochemical Impedance Spectroscopy (EIS) was performed on an AUTOLAB PGSTAT30 (Ecochemie, Netherlands), equipped with FRA module and with equivalent set-up as in the voltammetric measurements.

3. Results and discussion

3.1. Chemical and morphological analysis of CDs

All the synthesized modified CDs where analysed by elementary analysis in order to quantify the sulphur and nitrogen compositions (Table 1). The results confirm the correct modification of the graphitic CDs, showing an appropriate doping grade, around 10%; moreover, the table demonstrates the previous absence of S and N in the pristine material, as it corresponds.

By SEM analysis the morphology of the obtained *N*- and *S*-CDs (Fig. 1) could be visualized; the obtained images exhibit spherical shape and different degree of aggregations for *N*-CDs (Fig. 1B) and *S*-CDs (Fig. 1C) compared with the raw CDs (Fig. 1A). This fact can be explained by the different surface charge of modified carbon dots; *S*-CDs surface is populated by a higher concentration of sulphonic ($R–SO_3^-$) groups and *N*-CDs by amide/amine ($-CONH_2$/$-CNH_2$) protonable groups.

The size histograms, made from different images and for approximately 150 measurements for each material, show mean diameters equal to 18, 16 and 4 nm for CDs, *N*-CDs and *S*-CDs, respectively.

To support the stated doping, XPS analysis were performed with both *N*-CDs and *S*-CDs. Fig. 2 visualizes the different functional groups presented in both nano-dots. The main contribution in both nanoparticles, is assigned to C 1*s* composition and attributed to C–C/C–H at 284.9 eV (~83%), with small contributions related to C–O at 286 eV and carbonyl and carboxylic groups at 287.3 eV. *N*-CDs and *S*-CDs

Table 3
Summary table of calibration experiments for AA, SA and Cys for bare GC, graphite ink, CDs, *N*-CDs and *S*-CDs electrodes. All measurement carried out at same conditions and same range of concentrations.

	GC Electrode	Graphite Ink	CDs	*N*-CDs	*S*-CDs
Ascorbic Acid					
Peak potential (V)	0.32	0.32	0.32	0.42	0.32
Calibration line	$y = 1.82{\cdot}10^{-2}x + 4.26{\cdot}10^{-7}$	$y = 3.24{\cdot}10^{-2}x + 2.79{\cdot}10^{-6}$	$y = 2.62{\cdot}10^{-2}x + 1.24{\cdot}10^{-6}$	$y = 2.39{\cdot}10^{-2}x + 2.61{\cdot}10^{-6}$	$y = 2.07{\cdot}10^{-2}x + 2.13{\cdot}10^{-6}$
R^2	0.9995	0.9996	0.9999	0.9993	0.9997
LOD (μM)	101	88.7	20.7	121	78.0
Salicylic Acid					
Peak potential (V)	0.91	0.84	0.84	0.87	0.85
Calibration line	$y = 2.15{\cdot}10^{-2}x + 1.12{\cdot}10^{-6}$	$y = 3.55{\cdot}10^{-2}x + 2.72{\cdot}10^{-6}$	$y = 4.64{\cdot}10^{-2}x + 4.94{\cdot}10^{-6}$	$y = 3.85{\cdot}10^{-2}x + 3.34{\cdot}10^{-6}$	$y = 3.60{\cdot}10^{-2}x + 3.04{\cdot}10^{-6}$
R^2	0.9995	0.998	0.998	0.998	0.998
LOD (μM)	51.1	113	101	91.2	94.8
Cysteine					
Peak potential (V)	0.64	0.64	0.63	0.64	0.63
Calibration line	$y = 5.60{\cdot}10^{-3}x + 9.03{\cdot}10^{-7}$	$y = 2.01{\cdot}10^{-2}x + 9.33{\cdot}10^{-6}$	$y = 1.73{\cdot}10^{-2}x + 7.31{\cdot}10^{-6}$	$y = 1.43{\cdot}10^{-2}x + 7.29{\cdot}10^{-6}$	$y = 1.70{\cdot}10^{-2}x + 8.27{\cdot}10^{-6}$
R^2	0.987	0.970	0.970	0.950	0.972
LOD (μM)	287	420	427	548	407

showed the presence of amine/amide (NH_2/O═C–NH_2) at 400.2 eV for N 1*s* contribution (Fig. 2A) and sulphate/sulphonic (SO_4^{2-} (33%)/ R–SO_3^- (67%)) functional groups at 168.2 and 169.8 eV respectively, for S 2*p* contribution (Fig. 2B). O 1*s* signals showed two main contributions for C–O and O–C═O for *N*-CDs and an additional contribution for S═O in the case of *S*-CDs.

Mass spectra of *N*- and *S*-CDs have confirmed the composition of both nanoparticles, and they are presented in Fig. 3. Detected signals, their position and their identity are given in Table 2. Presented spectra are acquired by matrix-free approach, which was possible due to optical and semi-conductive properties of carbon dots. Signals were confirmed also by the spectra measured with organic matrices (data not shown), and according to the mechanism of information, in the case of *S*-carbon dots, the addition of protons and sodium/potassium was necessary for charge compensation of SO_3^- group on the surface of CDs and subsequent ionization. Less additional positive ions were required for the ionization of *N*-CDs. The number of carbon atoms was between 9 and 29, whereas in the spectra of *S*-CDs, a dimmer and a trimmer were detectable (at *m/z* 591.9 and at 887.9, respectively). They are most likely generated in the gas phase after the laser induced desorption and ionization, as detected for other analytes [49].

3.2. Electrochemical characterization

Since the CDs are highly conductive, they were tested and characterized onto electrode surfaces for they use as key transducer modifier material. The platform chosen for the performance of electric measurement was the glassy carbon electrode (GC) owing to their well-known characteristics and responses. The placement of CDs on the surface of these electrodes was carried out using polystyrene inks. The work herein has as predecessor article with pristine carbon CDs developed in the same group [40]. This study also used GC electrodes, which were modified via a drop casting method; in the present work, due to the water solubility of *N*-CDs and *S*-CDs, it was mandatory the use of an alternate method. For this reason, a conductive ink approach was attempted. The employed ink had a basis of polystyrene as polymeric part, graphite as bulk conductive material and mesitylene as solvent. To that suspension it was added a 10% w/w of modifier, in this case the CDs.

When XPS was used to inspect, not the CDs themselves, but the ink surfaces, prepared with the different doped and pristine CDs, no clear differences could be observed in the spectra, suggesting the doping atoms are embedded in the graphitic core; in the same sense, initial electrochemical evaluations were lacking clear signal and differentiation between the different variants, suggesting us an activation of the deposited ink was necessary in order to expose the reactive spots to the electrochemical processes and enhance the electro-transfer. There are multiple methods described in the bibliography for the activation of surfaces, most of them include the application of extreme potentials in presence of different solutions, for example, hydrogen peroxide or sulphuric acid [47,50]; on the other hand, other authors use solutions such as sodium hydroxide or simply phosphate buffer solutions [48,51]. The main conclusions of these works are the creation of new oxygenated groups which produce and increase of the electroactive area, another option that explain the results obtained in the activation process is the creation of new porous in the ink surface produced for the degradation of non conductive organic compounds.

On Fig. 4A, it can be observed the effect of the activation process, where increasing peaks appear and stabilize after ca. 10 cycles. In the same Figure, it also appears the signal of a bare GC electrode which did not present any major change. Additionally, the activation step was followed by electrochemical impedance spectroscopy (EIS); the measurements were carried out in $[Fe(CN)_6]^{3-/4-}$ between 0.5 MHz and 0.05 Hz with a sinusoidal voltage perturbation of 10 mV amplitude. In Fig. 4B and C, the EIS results for non activated and activated electrodes, respectively, are depicted. The Nyquist plots state equivalent results to those from cyclic voltammetry, since non-activated inks show a larger charge transfer resistance than the activated electrodes. Moreover, a bare GC electrode was measured in order to ensure the obtained results depend on the activation of the ink and not on any alteration on the GC electrode.

Given the depositing process is manually conducted, it was necessary to study its reproducibility and repeatability. For this, the active surface area of each electrode was calculated with the Randles-Sevcik equation and with use of the $[Fe(CN)_6]^{3-/4-}$ redox pair. By applying 6 different voltammetry scan rates (10, 20, 50, 100, 200 and 300 mV s^{-1}) it was obtained the following active areas (confidence interval calculated for 5 different days and 5 different depositions): 42.18 ± 0.06 mm^2 for pristine CDs ink, 29.19 ± 0.07 mm^2 for *S*-CDs ink, 43.94 ± 0.08 mm^2 for *N*-CDs ink, 30.62 ± 0.08 mm^2 for graphite ink and 15.24 ± 0.03 mm^2 for the bare GC electrode (geometrical diameter, Ø = 3 mm in all cases). The results demonstrate a high reproducibility of deposition and activation, 0.26% in the worst case, showing it is a robust modification technique. On the other hand, the activation step demonstrates a noticeable increase of the active area (ca. a factor of 3) in front of the bare GC electrode, leading this to higher current responses, markedly for the *N*-doped CDs. In the individual use of these produced electrodes, their specific reproducibility and repeatability values are 9.5% and 1%, respectively.

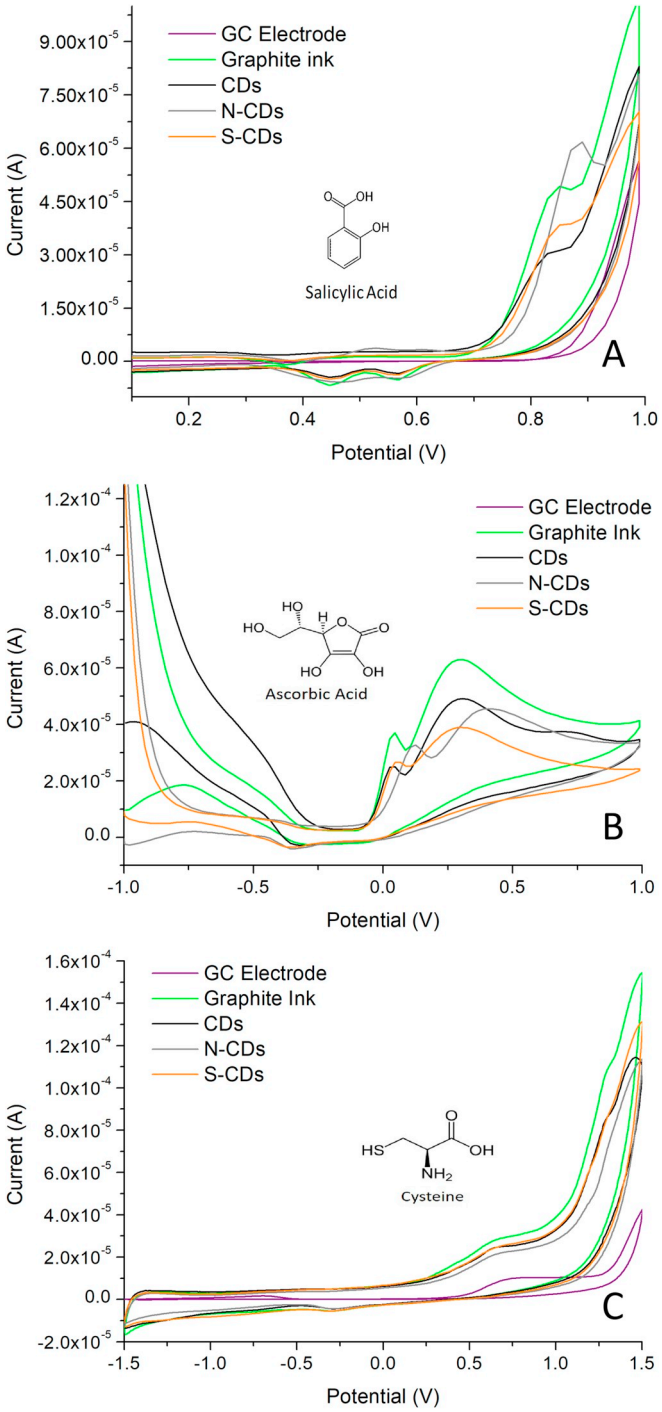

Fig. 5. Comparison of the cyclic voltammograms, at the same concentration of analyte, obtained from the 5 considered electrodes for (A) SA, (B) AA and (C) Cys.

3.3. Electrochemical measurements

Once a satisfactory method for integrating and immobilizing the CD modifiers was established, electrochemical measurements with different families of oxidizable organic compounds were performed. Specifically, the chosen analytes were Ascorbic acid (AA), Cysteine (CYS) and Salicylic Acid (SA), compounds that may be present in pharmaceutical compositions and also be used as food additives [52–54] The complexity to analyse them via standard electrochemical methods, due to extreme oxidation potentials and low defined peaks [55–57], makes of these three compounds interesting focus for study.

The results obtained for AA, SA and CYS, are summarized on Table 3. The values shown in the table indicate a clear improvement of the sensitivity with use of the CDs; the slopes of the modified electrodes vs. the bare GC electrode demonstrate a twice increase, most of the times. This signal increase can be also observed on Fig. 5, where the effect of specially the *N*-doped CDs demonstrates, in the SA oxidation, the improvements achieved. CYS is the compound interacting mostly with the *S*-CD modifier, probably through its own thiol moiety, presenting an increase of more than 3.5 times the current obtained for the bare glassy carbon electrode. This also demonstrates a good synergy between the inks and synthesized carbon dots. The better linearities of the measurements performed corresponded to AA and SA but not for CYS, as it is deduced from the correlation coefficients. Also, Table 3 allows observing that there are no other differences between the currents for the electrodes modified with the distinct inks, which lead us to affirm that the improvements in current are, in first instance, a result of the increase of the active surface.

But obviously, it is not only the increase of the current the benefit pursued with the modification of the carbon electrode; concretely, the catalytic effects on the potential are also as interesting as a further improvement in voltammetric measurements. And herein we can observe two of these examples. First on Fig. 5A, it is evident that the different modifiers decrease the potential for the oxidation of SA vs. the GCE, not only with reduction of the potential maximum, but also with a better definition of the peak.

As shown on Fig. 5C, and more clearly depicted on Fig. 6, a clear shift towards lower potential is observed in the case of the CD modified electrodes for AA determination. Particularly, the potentials are lowered ca. 200 mV, a relevant value. It is also important to notice the special effect on the AA oxidation signal, where the peak is unfolded in two overlapped peaks, which means the two different oxidations are better differentiated.

Finally, Fig. 7 shows a complete calibration, in this case corresponding to SA with the different electrodes. In this case, a higher signal with the pristine CDs is manifested, explained the electro-donation process by the presence on the CDs surface of organic moieties based in O functional groups, while comparable responses for the doped and standard graphite inks seem confirmed, the presence of amine and amide in *N*-CDs and sulfonyl organic groups decreased this electro-donor character of the doped N and *S*-CDs; it should be considered here that the enhancement to remark with SA are the catalytic effects, displayed in the reduction of the potential of the oxidation peaks, as commented above. Findings in consonance to these were found in studying the effects of doping to the electroanalytical properties of graphene-modified electrodes [58]. *N*-doping did not enhance currents whereas oxidation potentials where slightly decreased; in this interesting work, the clearer improvements were obtained with B-doped graphenes in terms of sensitivity, linearity and selectivity of response. From these findings, also supported partially by ours, graphene material (or CDs) doped with electron donating heteroatoms, both with N and S, would display slightly improved electrochemical performance for the tested oxidation reactions, and certain catalytic effect, while the highest improvements in all aspects would be originated by electron withdrawing heteroatoms. Further experimentation would be needed to confirm the effects with boron-doped CDs, while effect on reduction reactions are still to be verified.

A final reflection to be done with the scrutiny of the signals obtained, is that, as it is easily observed on the graphs, each modification produces different signal profiles, (this is mostly evident with the SA and AA cases) making it an exceptional property for a future application of carbon dots in studies of the electronic tongue type. Recalling the electronic tongue definition, this is “an analytical instrument comprising an electrode array of nonspecific, low-selective, stable and cross-sensitivity to different species” [59,60]. The nature of the signals obtained lead us to regard the developed materials as interesting transducer modifiers applied as sensors forming the array on electronic

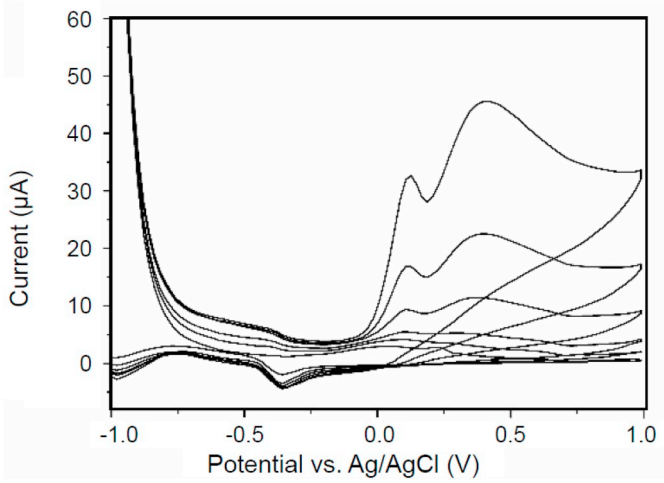

Fig. 6. Cyclic voltammograms obtained with AA when a *N*-CDs modified electrode is used for the measurement of different concentrations (0.002–3 mM) of the analyte.

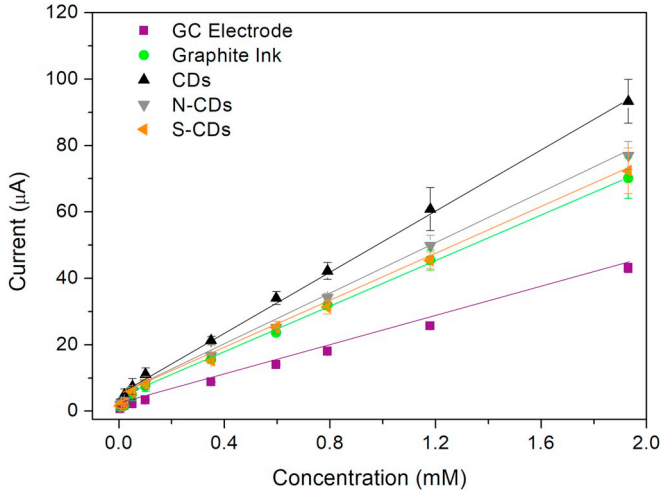

Fig. 7. Calibration curves for SA measured with GC electrode and Graphite ink, CDs, *N*-CDs and *S*-CDs GC modified electrodes. Error bars corresponding to three calibrations, made in different days.

tongues, as the starting point for its development is that the different sensors must produce differentiated signals for the different compounds studied. This point is clearly evident from Fig. 5, what proves the cross-sensitivity feature, and makes this a starting point to consider further work on this direction.

4. Conclusions

N- and *S*-doped carbon dots were successfully synthesized and characterized via SEM microscopy, MALDI TOF mass spectrometry, elementary analysis and XPS, in exploration of new nanotechnology-type modifiers for voltammetry. Synthesized *N*- and *S*- CDs were with regular shapes of nanoscale dimensions, and the modification of CDs was clearly shown by elemental analysis, mass spectrometry and XPS. In this respect, we have clearly demonstrated the potential of CDs and its derivates to catalyse the oxidation potential and the ability to provide different voltammetric profiles for the same compound, making them interesting and novel for their use in sensor arrays for electronic tongues.

The data show a reproducible modification method with use of a conductive ink-like preparation. The developed modification method is related with a remarkable active surface area which produces a clear enhancement of the current signal. Overall, the materials employed represent a remarkably green approach for obtaining and modifying electrochemical sensors. Tested compounds with these CDs inks modified electrodes were ascorbic acid, salicylic acid and cysteine, as generic oxidizable organic substances. All the compounds examined showed signal improvement in their cyclic voltammetric measurements. For example, signals of salicylic acid were shifted to lower potentials, what is a proof of the increase of the heterogeneous electron transfer rate and demonstrates an enhanced catalytic response. When comparing the different materials, the effect of the doping heteroatom on the response is more noticeable for *N*-CDs than for *S*-CDs, but both displayed better responses than the unmodified CDs, resulting on a two-fold increase of the response of the GCE.

Acknowledgments

The authors thank to the project CTQ2016-80170-P (MINECO, Spain). This work was also supported by FCT-Fundação para a Ciência e a Tecnologia through the CQM Base Fund - UIDB/00674/2020, and Programmatic Fund - UIDP/00674/2020, and by ARDITI-Agência Regional para o Desenvolvimento da Investigação Tecnologia e Inovação, through the project M1420-01-0145-FEDER-000005 - Centro de Química da Madeira - CQM+ (Madeira 14–20 Program). MdV thanks the support from program ICREA Academia. MBSE thanks to la Secretaria d'Universitats i Recerca del Departament d'Empreses i Coneixement de la Generalitat de Catalunya and to European Social Fund, European Union for a FI fellowship.

Appendix A. Supplementary data

Supplementary data to this article can be found online at https://doi.org/10.1016/j.talanta.2020.120806.

References

[1] X. Xu, R. Ray, Y. Gu, H.J. Ploehn, L. Gearheart, K. Raker, W.A. Scrivens, Electrophoretic analysis and purification of fluorescent single-walled carbon nanotube fragments, J. Am. Chem. Soc. 126 (2004) 12736–12737, https://doi.org/10.1021/ja040082h.
[2] J.C.G.E. da Silva, H.M.R. Gonçalves, Analytical and bioanalytical applications of carbon dots, TrAC Trends Anal. Chem. 30 (2011) 1327–1336, https://doi.org/10.1016/j.trac.2011.04.009.
[3] H. Li, Z. Kang, Y. Liu, S.-T. Lee, Carbon nanodots: synthesis, properties and applications, J. Mater. Chem. 22 (2012) 24230–24253, https://doi.org/10.1039/c2jm34690g.
[4] X. Sun, Y. Lei, Fluorescent carbon dots and their sensing applications, TrAC Trends Anal. Chem. 89 (2017) 163–180, https://doi.org/10.1016/j.trac.2017.02.001.
[5] S. Zhu, Q. Meng, L. Wang, J. Zhang, Y. Song, H. Jin, K. Zhang, H. Sun, H. Wang, B. Yang, Highly photoluminescent carbon dots for multicolor patterning, Sens. Bioimag. Angew. Chem. 125 (2013) 4045–4049, https://doi.org/10.1002/ange.201300519.
[6] A. Sachdev, P. Gopinath, Green synthesis of multifunctional carbon dots from coriander leaves and their potential application as antioxidants, sensors and bioimaging agents, Analyst 140 (2015) 4260–4269, https://doi.org/10.1039/c5an00454c.
[7] W. Lu, X. Qin, S. Liu, G. Chang, Y. Zhang, Y. Luo, A.M. Asiri, A.O. Al-Youbi, X. Sun, Economical, green synthesis of fluorescent carbon nanoparticles and their use as probes for sensitive and selective detection of mercury(II) ions, Anal. Chem. 84 (2012) 5351–5357, https://doi.org/10.1021/ac3007939.
[8] M. Algarra, M. Pérez-Martínez, M. Cifuentes-Rueda, J. Jiménez-Jiménez, J.C.G.E. da Silva, T.J. Bandosz, E. Rodríguez-Castellón, J.T.L. Navarrete, J. Casado, Carbon dots obtained using hydrothermal treatment of formaldehyde. Cell imaging in vitro, Nanoscale 6 (2014) 9071–9077, https://doi.org/10.1039/c4nr01585a.
[9] H. Shi, J. Wei, L. Qiang, X. Chen, X. Meng, Fluorescent carbon dots for bioimaging and biosensing applications, J. Biomed. Nanotechnol. 10 (2014) 2677–2699, https://doi.org/10.1166/jbn.2014.1881.
[10] A.H. Loo, Z. Sofer, D. Bouša, P. Ulbrich, A. Bonanni, M. Pumera, Carboxylic carbon quantum dots as a fluorescent sensing platform for DNA detection, ACS Appl. Mater. Interfaces 8 (2016) 1951–1957, https://doi.org/10.1021/acsami.5b10160.
[11] A. Rahy, C. Zhou, J. Zheng, S.Y. Park, M.J. Kim, I. Jang, S.J. Cho, D.J. Yang, Photoluminescent carbon nanoparticles produced by confined combustion of aromatic compounds, Carbon N. Y. 50 (2012) 1298–1302, https://doi.org/10.1016/j.carbon.2011.10.052.
[12] Q.-L. Zhao, Z.-L. Zhang, B.-H. Huang, J. Peng, M. Zhang, D.-W. Pang, Facile preparation of low cytotoxicity fluorescent carbon nanocrystals by electrooxidation of

graphite, Chem. Commun. (2008) 5116–5118, https://doi.org/10.1039/b812420e.
[13] S.C. Ray, A. Saha, N.R. Jana, R. Sarkar, Fluorescent carbon nanoparticles: synthesis, characterization, and bioimaging application, J. Phys. Chem. C 113 (2009) 18546–18551, https://doi.org/10.1021/jp905912n.
[14] S. Li, Z. Guo, Y. Zhang, W. Xue, Z. Liu, Blood compatibility evaluations of fluorescent carbon dots, ACS Appl. Mater. Interfaces 7 (2015) 19153–19162, https://doi.org/10.1021/acsami.5b04866.
[15] Y. Hou, Q. Lu, J. Deng, H. Li, Y. Zhang, One-pot electrochemical synthesis of functionalized fluorescent carbon dots and their selective sensing for mercury ion, Anal. Chim. Acta 866 (2015) 69–74, https://doi.org/10.1016/j.aca.2015.01.039.
[16] T. Atabaev, Doped carbon dots for sensing and bioimaging applications: a minireview, Nanomaterials 8 (2018) 342, https://doi.org/10.3390/nano8050342.
[17] M. Zhou, Z. Zhou, A. Gong, Y. Zhang, Q. Li, Synthesis of highly photoluminescent carbon dots via citric acid and Tris for iron(III) ions sensors and bioimaging, Talanta 143 (2015) 107–113, https://doi.org/10.1016/j.talanta.2015.04.015.
[18] Y. Du, S. Guo, Chemically doped fluorescent carbon and graphene quantum dots for bioimaging, sensor, catalytic and photoelectronic applications, Nanoscale 8 (2016) 2532–2543, https://doi.org/10.1039/c5nr07579c.
[19] S. Chaudhary, A. Umar, K.K. Bhasin, S. Singh, Applications of carbon dots in nanomedicine, J. Biomed. Nanotechnol. 13 (2017) 591–637, https://doi.org/10.1166/jbn.2017.2390.
[20] X. Lin, G. Gao, L. Zheng, Y. Chi, G. Chen, Encapsulation of strongly fluorescent carbon quantum dots in metal-organic frameworks for enhancing chemical sensing, Anal. Chem. 86 (2013) 1223–1228, https://doi.org/10.1021/ac403536a.
[21] N.A. Travlou, D.A. Giannakoudakis, M. Algarra, A.M. Labella, E. Rodríguez-Castellón, T.J. Bandosz, S- and N-doped carbon quantum dots: surface chemistry dependent antibacterial activity, Carbon N. Y. 135 (2018) 104–111, https://doi.org/10.1016/J.CARBON.2018.04.018.
[22] J. Praneerad, N. Thongsai, P. Supchocksoonthorn, S. Kladsomboon, P. Paoprasert, Multipurpose sensing applications of biocompatible radish-derived carbon dots as Cu2+ and acetic acid vapor sensors, Spectrochim. Acta Part A Mol. Biomol. Spectrosc. 211 (2019) 59–70, https://doi.org/10.1016/j.saa.2018.11.049.
[23] Y. Chen, D. Gao, H. Bai, H. Liu, S. Lin, Y. Jiang, Carbon dots and 9AA as a binary matrix for the detection of small molecules by matrix-assisted laser desorption/ionization mass spectrometry, J. Am. Soc. Mass Spectrom. 27 (2016) 1227–1235, https://doi.org/10.1007/s13361-016-1396-y.
[24] M.S. Khan, M.L. Bhaisare, S. Pandey, A. Talib, S.-M. Wu, S.K. Kailasa, H.-F. Wu, Exploring the ability of water soluble carbon dots as matrix for detecting neurological disorders using MALDI-TOF MS, Int. J. Mass Spectrom. 393 (2015) 25–33, https://doi.org/10.1016/j.ijms.2015.10.007.
[25] J. Zhou, X. Shan, J. Ma, Y. Gu, Z. Qian, J. Chen, H. Feng, Facile synthesis of P-doped carbon quantum dots with highly efficient photoluminescence, RSC Adv. 4 (2014) 5465–5468, https://doi.org/10.1039/c3ra45294h.
[26] Y. Dong, H. Pang, H. Bin Yang, C. Guo, J. Shao, Y. Chi, C.M. Li, T. Yu, Carbon-based dots Co-doped with nitrogen and sulfur for high quantum yield and excitation-independent emission, Angew. Chem. Int. Ed. 52 (2013) 7800–7804, https://doi.org/10.1002/anie.201301114.
[27] Q. Xu, P. Pu, J. Zhao, C. Dong, C. Gao, Y. Chen, J. Chen, Y. Liu, H. Zhou, Preparation of highly photoluminescent sulfur-doped carbon dots for Fe(iii) detection, J. Mater. Chem. A. 3 (2015) 542–546, https://doi.org/10.1039/c4ta05483k.
[28] Z. Lin, J. Wu, Y. Dong, P. Xie, Y. Zhang, Z. Cai, Nitrogen and sulfur Co-doped carbon-dot-assisted laser desorption/ionization time-of-flight mass spectrometry imaging for profiling bisphenol S distribution in mouse tissues, Anal. Chem. 90 (2018) 10872–10880, https://doi.org/10.1021/acs.analchem.8b02362.
[29] Y. Jiang, B. Wang, F. Meng, Y. Cheng, C. Zhu, Microwave-assisted preparation of N-doped carbon dots as a biosensor for electrochemical dopamine detection, J. Colloid Interface Sci. 452 (2015) 199–202, https://doi.org/10.1016/j.jcis.2015.04.016.
[30] X. Teng, C. Ma, C. Ge, M. Yan, J. Yang, Y. Zhang, P.C. Morais, H. Bi, Green synthesis of nitrogen-doped carbon dots from konjac flour with “off-on” fluorescence by Fe3+ and L-lysine for bioimaging, J. Mater. Chem. B. 2 (2014) 4631–4639, https://doi.org/10.1039/c4tb00368c.
[31] B.B. Campos, C. Abellán, M. Zougagh, J. Jimenez-Jimenez, E. Rodríguez-Castellón, J.C.G.E. da Silva, A. Ríos, M. Algarra, Fluorescent chemosensor for pyridine based on N-doped carbon dots, J. Colloid Interface Sci. 458 (2015) 209–216, https://doi.org/10.1016/j.jcis.2015.07.053.
[32] H. Liu, Y. Zhang, J.H. Liu, P. Hou, J. Zhou, C.Z. Huang, Preparation of nitrogen-doped carbon dots with high quantum yield from Bombyx mori silk for Fe(iii) ions detection, RSC Adv. 7 (2017) 50584–50590, https://doi.org/10.1039/c7ra10130a.
[33] M.Y. Emran, M.A. Shenashen, A.A. Abdelwahab, M. Abdelmottaleb, S.A. El-Safty, Facile synthesis of microporous sulfur-doped carbon spheres as electrodes for ultrasensitive detection of ascorbic acid in food and pharmaceutical products, New J. Chem. 42 (2018) 5037–5044, https://doi.org/10.1039/c7nj05047j.
[34] H. Liu, Y. Zhang, C. Huang, Development of nitrogen and sulfur-doped carbon dots for cellular imaging, J. Pharm. Anal. 9 (2019) 127–132, https://doi.org/10.1016/j.jpha.2018.10.001.
[35] Y. Wang, L. Yan, G. Ji, C. Wang, H. Gu, Q. Luo, Q. Chen, L. Chen, Y. Yang, C.-Q. Ma, X. Liu, Synthesis of N,S-doped carbon quantum dots for use in organic solar cells as the ZnO modifier to eliminate the light-soaking effect, ACS Appl. Mater. Interfaces 11 (2018) 2243–2253, https://doi.org/10.1021/acsami.8b17128.
[36] C. Hu, M. Li, J. Qiu, Y.-P. Sun, Design and fabrication of carbon dots for energy conversion and storage, Chem. Soc. Rev. 48 (2019) 2315–2337, https://doi.org/10.1039/c8cs00750k.
[37] S. Campuzano, P. Yáñez-Sedeño, J.M. Pingarrón, Carbon dots and graphene quantum dots in electrochemical biosensing, Nanomaterials 9 (2019) 634, https://doi.org/10.3390/nano9040634.
[38] M. Li, T. Chen, J.J. Gooding, J. Liu, Review of carbon and graphene quantum dots for sensing, ACS Sens. 4 (2019) 1732–1748, https://doi.org/10.1021/acssensors.9b00514.
[39] H.V. Nguyen, L. Richtera, A. Moulick, K. Xhaxhiu, J. Kudr, N. Cernei, H. Polanska, Z. Heger, M. Masarik, P. Kopel, M. Stiborova, T. Eckschlager, V. Adam, R. Kizek, Electrochemical sensing of etoposide using carbon quantum dot modified glassy carbon electrode, Analyst 141 (2016) 2665–2675, https://doi.org/10.1039/c5an02476e.
[40] M. Algarra, A. González-Calabuig, K. Radotić, D. Mutavdzic, C.O. Ania, J.M. Lázaro-Martínez, J. Jiménez-Jiménez, E. Rodrìguez-Castellón, M. del Valle, Enhanced electrochemical response of carbon quantum dot modified electrodes, Talanta 178 (2018) 679–685, https://doi.org/10.1016/j.talanta.2017.09.082.
[41] J. Tang, Simultaneous determination of hydroquinone and catechol using carbon glass electrode modified with graphene quantum dots, Int. J. Electrochem. Sci. (2018) 11250–11262, https://doi.org/10.20964/2018.11.52.
[42] S.S. Shankar, R.M. Shereema, V. Ramachandran, T.V. Sruthi, V.B.S. Kumar, R.B. Rakhi, Carbon quantum dot-modified carbon paste electrode-based sensor for selective and sensitive determination of adrenaline, ACS Omega 4 (2019) 7903–7910, https://doi.org/10.1021/acsomega.9b00230.
[43] S. Baluta, A. Lesiak, J. Cabaj, Graphene quantum dots-based electrochemical biosensor for catecholamine neurotransmitters detection, Electroanalysis 30 (2018) 1781–1790, https://doi.org/10.1002/elan.201700825.
[44] W. Chen, W. Weng, X. Niu, X. Li, Y. Men, W. Sun, G. Li, L. Dong, Boron-doped Graphene quantum dots modified electrode for electrochemistry and electrocatalysis of hemoglobin, J. Electroanal. Chem. 823 (2018) 137–145, https://doi.org/10.1016/j.jelechem.2018.06.001.
[45] G. Muthusankar, R. Sasikumar, S.-M. Chen, G. Gopu, N. Sengottuvelan, S.-P. Rwei, Electrochemical synthesis of nitrogen-doped carbon quantum dots decorated copper oxide for the sensitive and selective detection of non-steroidal anti-inflammatory drug in berries, J. Colloid Interface Sci. 523 (2018) 191–200, https://doi.org/10.1016/j.jcis.2018.03.095.
[46] L. Fu, A. Wang, G. Lai, C.-T. Lin, J. Yu, A. Yu, Z. Liu, K. Xie, W. Su, A glassy carbon electrode modified with N-doped carbon dots for improved detection of hydrogen peroxide and paracetamol, Microchim. Acta. 185 (2018) 87, https://doi.org/10.1007/s00604-017-2646-9.
[47] M.I. González-Sánchez, B. Gómez-Monedero, J. Agrisuelas, J. Iniesta, E. Valero, Highly activated screen-printed carbon electrodes by electrochemical treatment with hydrogen peroxide, Electrochem. Commun. 91 (2018) 36–40, https://doi.org/10.1016/J.ELECOM.2018.05.002.
[48] J. Wang, M. Pedrero, H. Sakslund, O. Hammerich, J. Pingarron, Electrochemical activation of screen-printed carbon strips, Analyst 21 (1996) 345–350.
[49] M. Petković, J. Schiller, M. Müller, R.S.K. Arnold, J. Arnhold, Detection of adducts with matrix clusters in the positive and negative ion mode MALDI-TOF mass spectra of phospholipids, Zeitschrift Für Naturforsch. B. 64 (2009) 331–334, https://doi.org/10.1515/znb-2009-0314.
[50] K. Shi, K.K. Shiu, Determination of uric acid at electrochemically activated glassy carbon electrode, Electroanalysis 13 (2001) 1319–1325, https://doi.org/10.1002/1521-4109(200111)13:16<1319::AID-ELAN1319>3.0.CO;2-C.
[51] D. Pan, S. Rong, G. Zhang, Y. Zhang, Q. Zhou, F. Liu, M. Li, D. Chang, H. Pan, Amperometric determination of dopamine using activated screen-printed carbon electrodes, Electrochemistry 83 (2015) 725–729, https://doi.org/10.5796/electrochemistry.83.725.
[52] J.F.I. Gregory, Ascorbic acid bioavailability in foods and supplements, Nutr. Rev. 51 (2009) 301–303, https://doi.org/10.1111/j.1753-4887.1993.tb03059.x.
[53] S. Schwimmer, D.G. Guadagni, Cysteine induced odor intensification in onions and other foods, J. Food Sci. 32 (1967) 405–408, https://doi.org/10.1111/j.1365-2621.1967.tb09696.x.
[54] J. Radtke, J. Linseisen, G. Wolfram, Phenolsäurezufuhr Erwachsener in einem bayerischen Teilkollektiv der Nationalen Verzehrsstudie, Eur. J. Nutr. 37 (1998) 190–197, https://doi.org/10.1007/s003940050016.
[55] F. Cao, Y. Huang, F. Wang, D. Kwak, Q. Dong, D. Song, J. Zeng, Y. Lei, A high-performance electrochemical sensor for biologically meaningful l-cysteine based on a new nanostructured l-cysteine electrocatalyst, Anal. Chim. Acta 1019 (2018) 103–110, https://doi.org/10.1016/j.aca.2018.02.048.
[56] M. Bonet-San-Emeterio, A. González, M. del Valle, Artificial neural networks for the resolution of dopamine and serotonin complex mixtures using a graphene-modified carbon electrode, Electroanalysis 31 (2019) 390–397, https://doi.org/10.1002/elan.201800525.
[57] D. Evans, J.P. Hart, G. Rees, Voltammetric behaviour of salicylic acid at a glassy carbon electrode and its determination in serum using liquid chromatography with amperometric detection, Analyst 116 (1991) 803–806, https://doi.org/10.1039/an9911600803.
[58] K.H. Hui, A. Ambrosi, Z. Sofer, M. Pumera, A. Bonanni, The dopant type and amount governs the electrochemical performance of graphene platforms for the antioxidant activity quantification, Nanoscale 7 (2015) 9040–9045, https://doi.org/10.1039/c5nr01045d.
[59] Y. Vlasov, A. Legin, A. Rudnitskaya, C. Di Natale, A. D’Amico, Nonspecific sensor arrays (“electronic tongue”) for chemical analysis of liquids (IUPAC Technical Report), Pure Appl. Chem. 77 (2005) 1965–1983, https://doi.org/10.1351/pac200577111965.
[60] M. del Valle, Bioinspired Sensor Systems, Sensors 11 (2011) 10180–10186, https://doi.org/10.3390/s111110180.